Photosynthesis inhibition during gas exchange oscillations in ABA-treated *Helianthus annuus*: relative role of stomatal patchiness and leaf carboxylation capacity

J. ŠANTRŮČEK[*,**,+], M. HRONKOVÁ[*,**], J. KVĚTOŇ[*,**], and R.F. SAGE[***]

Department of Photosynthesis, Institute of Plant Molecular Biology, Academy of Sciences of the Czech Republic, Branišovská 31, CZ-370 05 České Budějovice, Czech Republic[*]
The University of South Bohemia, Faculty of Biology and Institute of Physical Biology, Photosynthesis Research Centre, CZ-370 05 České Budějovice, Czech Republic[**]
Department of Botany, University of Toronto, 25 Willcocks Street, Toronto, Ontario M5S 3B2, Canada[***]

Abstract

Environmental factors that induce spatial heterogeneity of stomatal conductance, g_s, called stomatal patchiness, also reduce the photochemical capacity of CO_2 fixation, yet current methods cannot distinguish between the relative effect of stomatal patchiness and biochemical limitations on photosynthetic capacity. We evaluate effects of stomatal patchiness and the biochemical capacity of CO_2 fixation on the sensitivity of net photosynthetic rate (P_N) to stomatal conductance (g_s), θ ($\theta = \delta P_N/\delta g_s$). A qualitative model shows that stomatal patchiness increases the sensitivity θ while reduced biochemical capacity of CO_2 fixation lowers θ. We used this feature to distinguish between stomatal patchiness and mesophyll impairments in the photochemistry of CO_2 fixation. We compared gas exchange of sunflower (*Helianthus annuus* L.) plants grown in a growth chamber and fed abscisic acid, ABA (10^{-5} M), for 10 d with control plants (–ABA). P_N and g_s oscillated more frequently in ABA-treated than in control plants when the leaves were placed into the leaf chamber and exposed to a dry atmosphere. When compared with the initial CO_2 response measured at the beginning of the treatment (day zero), both ABA and control leaves showed reduced P_N at particular sub-stomatal CO_2 concentration (c_i) during the oscillations. A lower reduction of P_N at particular g_s indicated overestimation of c_i due to stomatal patchiness and/or omitted cuticular conductance, g_c. The initial period of damp oscillation was characterised by inhibition of chloroplast processes while stomatal patchiness prevailed at the steady state of gas exchange. The sensitivity θ remained at the original pre-treatment values at high g_s in both ABA and control plants. At low g_s, θ decreased in ABA-treated plants indicating an ABA-induced impairment of chloroplast processes. In control plants, g_c neglected in the calculation of g_s was the likely reason for apparent depression of photosynthesis at low g_s.

Additional key words: abscisic acid; CO_2 response; cuticular conductance; stomatal conductance; sunflower; transpiration.

Introduction

Within leaves, the control over photosynthetic carbon fixation can be partitioned into biochemical and diffusional components. Biochemical components can in turn be sub-divided into ribulose-1,5-bisphosphate carboxylase/oxygenase (RuBPCO) and the capacity for RuBP regeneration (Farquhar *et al.* 1980). Diffusional components are sub-divided into stomatal, mesophyll, and boundary layer functions. Of the diffusional control points, the stomatal component is most important because the guard cells are the means by which plants regulate diffusional control. The effect of stomata is normally indexed by stomatal conductance, g_s, parameter that

---

Received 20 January 2003, *accepted* 7 May 2003.
[+]Corresponding author; fax: +420-38-777 2371; e-mail: jsan@umbr.cas.cz
Abbreviations: c_a, ambient CO_2 concentration; c_i, CO_2 concentration in sub-stomatal cavity; E, transpiration rate; g_c, cuticular conductance; g_s, stomatal conductance; K_c and K_o, Michaelis-Menten constants for CO_2 and O_2, respectively; o, O_2 concentration in chloroplasts; O, oxygen-dependent parameter of CO_2 fixation [$O = K_c\ (1 + o/K_o)$]; P_N, net photosynthetic rate; R_D, dark respiration; RuBPCO, ribulose-1,5-bisphosphate carboxylase/oxygenase; V_{cmax}, maximum rate of carboxylation; *indexes*: $|_{ci}$, expressed at particular c_i; $_{gs}$, expressed at particular g_s; $_b$, caused by non-stomatal (biochemical) factors; $_p$, caused by stomatal patchiness; $_t$, total; Δ..., change in …; θ, slope of P_N *vs.* g_s ($\theta = \delta P_N/\delta g_s$); Γ, CO_2 compensation concentration without respiration.
Acknowledgements: This work was partly supported by Grant Agency of the Czech Republic (grant No. 206/00/162) and by the grants of the Ministry of Education of the Czech Republic (MSMT 123100004, LN00A141). J.S. thanks the Research School of Biological Sciences at the Australian National University, Canberra for a stimulating research environment and ideas helping us to start this work.

integrates the effect of many stomata over the surface of the leaf. A key assumption in using stomatal conductance to assess diffusional control is that g_s is uniform over the surface of the leaf (Laisk 1983, Farquhar 1989, Van Kraalinger 1990). This requires that stomata behave uniformly in response to environmental variation. It has, however, been recognised that individual stomata can exhibit unique, independent responses (Lange *et al.* 1971, Kaiser and Kappen 2001). As well, adjacent patches of stomata can behave independently, creating regions across the leaf surface of heterogeneous g_s (for reviews see Terashima 1992, Pospíšilová and Šantrůček 1997, Weyers and Lawson 1997, Mott and Buckley 1998). This can alter photosynthetic responses and the pattern of diffusional control in a manner that is often difficult to detect with standard gas exchange techniques. Operationally, this phenomenon has been termed stomatal patchiness.

An interesting feature of stomatal patchiness is a co-ordination of stomatal behaviour at the small spatial scale of the patch, but poor co-ordination across the leaf. Patch closure is commonly observed after abiotic stress such as soil drought and salinity, increased evaporative demand (Sharkey and Seemann 1989, Downton *et al.* 1990, Haefner *et al.* 1997), and artificially, following ABA feeding to the leaf (Terashima *et al.* 1988, Hirasawa *et al.* 1995, Mott 1995). The mechanism of patch dynamics is uncertain, although recent work indicates hydraulic dynamics across the epidermis play an important role (Buckley and Mott 2000).

Alternatively, there is the possibility that stomatal patchiness is a secondary response to a heterogeneous pattern in the photosynthetic biochemistry of mesophyll cells (Osmond *et al.* 1999). In non-stressed conditions, g_s responds in proportion to changes in photosynthetic activity in order to maintain a constant supply of CO_2 to the mesophyll. Patchy reduction in chloroplast activity could in turn induce a patchy pattern of g_s. Discriminating between patchiness caused by stomatal closure, as opposed to patchy mesophyll behaviour, is necessary if the contribution of biochemical and diffusional control to the stress response of photosynthesis is to be understood.

In this report, we present a new way to evaluate the contribution of stomatal patchiness, *versus* mesophyll impairment, to photosynthesis depressions caused by ABA exposure or other stress treatment. The technique consists of first modelling the sensitivity of photosynthesis to g_s, $\theta = \delta P_N/\delta g_s$, as affected by stomatal and/or mesophyll patchiness. Then the gas exchange dynamics of θ are analysed during oscillations of the CO_2 and H_2O exchange signals from ABA fed and control leaves.

Model

Effect of stomatal patchiness on P_N: Under conditions when the spatial heterogeneity of g_s is the only variable, stomatal patchiness (expressed as v_g, the coefficient of variation of g_s) reduces the whole-leaf P_N, even if the mean g_s remains constant (Fig. 1). For the leaf with uniform g_s, P_N is described by the solid curve in Fig. 1. For a patchy leaf, P_N declines by ΔP_{Np} even if $\bar{g}_s$ remains unchanged. When, for example, one half of the leaf has a near-zero conductance (g_{s2}) and the second half has high conductance (g_{s1}), the arithmetical mean of two corresponding P_N values will be lower by ΔP_{Np}. This concept assumes that mesophyll capacity of CO_2 fixation remains unchanged in patchy leaves (Terashima *et al.* 1988, Cheeseman 1991, Buckley *et al.* 1997). Every pattern of patchiness (a statistical distribution of g_s with $vg_{s1} > 0$) will cause depression of P_N by a particular value of ΔP_{Np} provided the P_N *vs.* g_s curve has negative curvature.

Effect of carboxylation capacity on P_N: Here, we evaluate the effect of variations in mesophyll carboxylation capacity on P_N, assuming g_s is constant. The biochemistry of CO_2 fixation is incorporated into robust models of photosynthesis (Farquhar *et al.* 1980, Caemmerer and Farquhar 1981, see also Eq. A1 in Appendix). The maximum rate of carboxylation, V_{cmax}, is proportional to the amount and activation state of RuBPCO. RuBPCO capacity is a major control over the biochemical capacity of photosynthesis at saturation irradiance and CO_2 concentrations below the current ambient of 370 μmol(CO_2) mol^{-1}. In particular, the initial slope of P_N *versus* CO_2 concentration in the chloroplast stroma is a function of RuBPCO capacity at saturating irradiance. Having the possibility to derive the slopes of the P_N *versus* c_i for individual patches, we could obtain multiple patch-specific estimates of V_{cmax}. Hence, the leaves with mesophyll patchiness show spatially variable V_{cmax}. We will treat V_{cmax} as a spatially uniform magnitude in the following paragraphs and consider the effect of patchy mesophyll in the Discussion.

Assuming g_s is constant, what is the relation between V_{cmax} and P_N? A decline in V_{cmax} causes a drop of P_N (Eq. A1 in the Appendix, called the 'demand function') (Farquhar and Sharkey 1982). If g_s is uniform and invariable, c_i rises linearly with the reduction in P_N provided ambient CO_2 concentration, c_a, does not change (see the diffusion relation called supply function in Eq. A2 in Appendix). The combination of the demand function and supply function (Eqs. A1 and A2) offsets c_i. Thus, the CO_2 response of photosynthesis can be mathematically transformed into the $P_N(g_s)$ relationship with the parameters V_{cmax}, O, and Γ sufficient to yield P_N for particular c_a and g_s (Eq. A3 in Appendix). Manipulating g_s and keeping c_a, V_{cmax}, O, and Γ constant, we obtain the $P_N(g_s)$

curve which shows the partial effect of stomatal patchiness on photosynthesis (Fig. 1). In turn, manipulating V_{cmax} in Eq. A3 while keeping g_s, c_a, O, and Γ constant, the partial effect of mesophyll capacity (V_{cmax}) on P_N can be assessed. P_N *versus* V_{cmax} yields a concave curve similar to $P_N(g_s)$ curve in Fig. 1.

V_{cmax} can vary with environmental stress (Wullschleger 1993). Provided that V_{cmax} of the whole leaf can be lowered by a stress factor, P_N will be depressed by this biochemical impairment independently of stomatal patchiness. This situation is shown by the dashed curve in Fig. 1. The V_{cmax} depression, ΔV_{cmax}, was adjusted here so that the biochemical ($_b$) depression of P_N, ΔP_{Nb}, was equal to ΔP_{Np}.

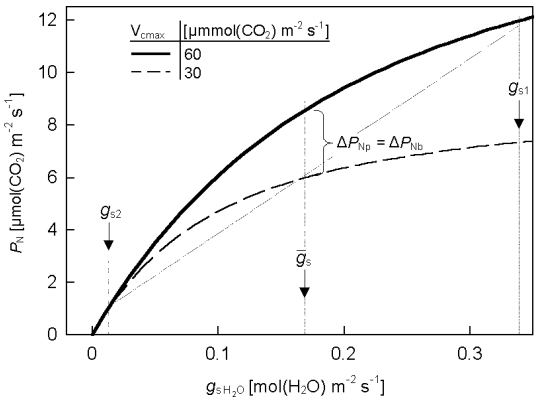

Fig. 1. A diagram showing how the photosynthetic rate P_N of a non-stressed leaf having uniform stomatal conductance $\bar{g}_s$ drops by the ΔP_{Np} value in a patchy leaf when one half of stomata population closes (g_{s2}) and the other half opens to (g_{s1}) so that $\bar{g}_s$ remains unchanged. The new rate of photosynthesis affected by patchiness is then an arithmetic mean of P_N at g_{s1} and P_N at g_{s2} (Terashima *et al*. 1988, Farquhar 1989). The $P_N(g_s)$ relation of the non-stressed leaf with carboxylation capacity V_{cmax} = 60 μmol(CO_2) m^{-2} s^{-1} is represented by the solid curve; the dashed curve shows the P_N response to g_s when V_{cmax} is one half of its value in the non-stressed leaf. If g_s is uniformly distributed and has the $\bar{g}_s$ value, then the biochemical depression of photosynthesis ΔP_{Nb} equals ΔP_{Np}. The curves were calculated using Eq. A3 (Appendix) where O = 245 μmol(CO_2) mol^{-1}, c_a = 180 μmol(CO_2) mol^{-1}, and Γ = 50 μmol(CO_2) mol^{-1} and g_s varied between 0 and 0.22 mol(CO_2) m^{-2} s^{-1} (see Eq. A1 in Appendix). The results are plotted *versus* g_s in mol(H_2O) m^{-2} s^{-1}.

Effects of stomatal patchiness and carboxylation capacity on sensitivity of P_N to changing g_s: The sensitivity of P_N to changes in g_s, $\delta P_N/\delta g_s$, referred to as θ hereafter, is an important parameter for optimisation of carbon gain. Geometrically, it represents the slope of the curve in Fig. 1, that is, the first derivative of the P_N *vs.* g_s curve. Further, when θ is plotted against g_s, a non-linear response with maximum at zero conductance is obtained (Fig. 2). The occurrence of stomatal patchiness increases the original θ by $\Delta\theta_p$, while a decline in mesophyll capacity (*the dashed curve* in Fig. 2) lowers the original θ by $\Delta\theta_b$. The increase is due to the shape of θ when plotted *versus* g_s: the shape 'concave-from-above' increases the average θ value at a particular g_s when g_s becomes heterogeneous. In opposite, the decrease in θ is obtained when g_s stays invariable but the average leaf V_{cmax} is reduced. (Subscripts *p* and *b* in Figs. 1 and 2 indicate patchiness and carboxylation activity, respectively.) Thus, the total change of the sensitivity, $\Delta\theta_t$ equals

$$\Delta\theta_t = \Delta\theta_p + \Delta\theta_b = (\theta_p - \theta) + (\theta_b - \theta) \quad (1)$$

This parameter shows the main reason for the photosynthesis depression: when $\Delta\theta_t$ is positive, the patchiness-induced decline in P_N is greater than the biochemically-induced reduction. When $\Delta\theta_t$ is negative, the opposite is true. If the mesophyll inhibition of $\Delta\theta_b$ is offset by the patchiness-induced rise in $\Delta\theta_p$, the total change $\Delta\theta_t$ equals zero.

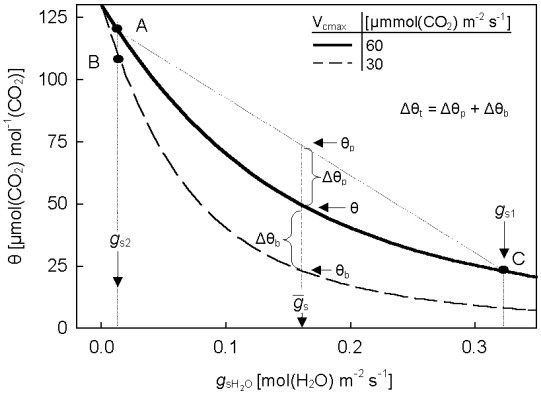

Fig. 2. Sensitivity of photosynthesis to changes in stomatal conductance, g_s ($\theta = \delta P_N/\delta g_s$) calculated as a derivative of the curves in Fig. 1 (using Eqs. A4a, A4b in Appendix and taking g_{sCO2}) and plotted *versus* stomatal conductance g_{sH2O}. The sensitivity value in a non-stressed leaf (*solid curve*) rises by $\Delta\theta_p$ if stomata became patchy and drops by $\Delta\theta_b$ by a 50 % depression in carboxylation capacity. The total change of the sensitivity after a non-specified stress treatment, $\Delta\theta_t$, is a sum of both partial components. The letters A and C refer to the operating points in the low-g_s area and high-g_s area of the non-stressed leaf; B is the operating point in the low-g_s region after its mesophyll capacity has been reduced. For further explanation of A, B, and C—see mesophyll patchiness in Discussion.

How can the total change in θ be measured? Although the partial effects of stomatal patchiness and mesophyll impairment are not initially known, θ can be measured before and after a stress treatment that causes photosynthetic depressions. Pre-stress θ values can be obtained using Eqs. A4a and A4b (in Appendix) and parameters of the $P_N(c_i)$ curve measured prior the stress (ABA) treatment. Post-stress values of θ, θ_t, can be estimated from variations of g_s and photosynthesis induced experimentally. Assuming that the g_s and P_N variations do not alter the main cause of photosynthesis depression, the difference

between θ_t and the pre-stress θ reveals the cause. We calculated θ_t from periodic changes of g_s and P_N with time (oscillations). Oscillations can be induced using plants that are suddenly exposed to dry and low-CO_2 air.

The total change in sensitivity can then be calculated as a difference between the post-ABA and pre-ABA values (see Eq. A5 in Appendix for definition of θ_t):

$$\Delta\theta_t = \theta_t - \theta \quad (2)$$

Materials and methods

Plants: Sunflower (*Helianthus annuus* L.) plants were grown from seeds in plastic 1 000 cm^3 pots filled with perlite soaked with a full-strength IBP nutrient solution (Table 1). Pots were placed in a 2 500 cm^3 container of the IBP solution which was renewed every second day. The plants were grown in a growth chamber (*Sherer*, USA) at day/night air temperatures of 23/15 °C and irradiance of 300–400 μmol(photon) m^{-2} s^{-1} for 16 h per day. At the stage of the 6th fully-developed leaf, ABA (±*cis-trans*-abscisic acid, *Sigma-Aldrich*, Germany) was added to the nutrient solution (10^{-5} M ABA in the final solution) of four plants. Three other plants with no ABA exposure were used as a control.

Table 1. International Biological Program (IBP) nutrient solution. [A]From the Fe stock solution 0.5 cm^3 were added to each litre of final nutrient solution.

Macroelements	Concentration [mM]	Microelements	Concentration [mM]
$Ca(NO_3)_2$	4.00	$MnSO_4 \times 4\ H_2O$	0.0100
KNO_3	4.00	$CuSO_4 \times 5\ H_2O$	0.0005
$MgSO_4 \times 7\ H_2O$	1.50	$ZnSO_4 \times 7\ H_2O$	0.0010
$NaH_2PO_4 \times 2\ H_2O$	1.33	H_3BO_3	0.0300
		NaCl	0.1000
Fe EDTA (stock solution)[A] [kg m^{-3}]:		$Na_2MoO_4 \times 2\ H_2O$	0.0005
EDTA	29.7		
KOH	16.8		
$FeSO_4 \times 7\ H_2O$	27.8		

CO_2 and water exchange: Prior to ABA treatment (day zero), the $P_N(c_i)$ curves had been measured on the 6th leaf of each plant using a photosynthetic gas-exchange system (*LI-6400P*, *Li-Cor*, USA) starting at an ambient CO_2 of 350 μmol(CO_2) mol^{-1}, followed by 50, 100, 180, 280, 350, 600, and 1 200 μmol(CO_2) mol^{-1}. The leaf temperature was 25 °C and irradiance 500 μmol(photon) m^{-2} s^{-1}. On the fourth to tenth day after the ABA supply, gas exchange of the same leaves was re-determined at a c_a of 180 or 280 μmol(CO_2) mol^{-1} for 40 to 120 min after the leaf had been closed into the leaf chamber. The leaf chamber was preconditioned so that the leaf could experience the same conditions (irradiance, leaf temperature, c_a) as during the CO_2 response measurement. There had been no period of darkness before the leaf was accommodated in the leaf chamber. The input air humidity was close to zero during these measurements, giving the leaf-to-air vapour pressure difference of 1.5–2.1 kPa. Both ABA-treated and control plants were investigated in this way. Low-CO_2 and dry air induced oscillations of g_s and P_N in ABA fed plants regularly and several times also in control plants. The 60 s or 30 s averages of P_N, transpiration rate (E), c_i, g_s, and other parameters were recorded for 40–120 min after initiation of oscillations. Thirteen time courses from 4 ABA plants and 7 courses from 3 control plants were measured. We analyse the 120 min record obtained at c_a 180 μmol(CO_2) mol^{-1} with an ABA plant first and then show the results pooled from all ABA and all control plants.

Estimation of the sensitivity of P_N to changes in g_s: We constructed the pre-stress $P_N(g_s)$ relation (Eq. A3 in Appendix) for each measured leaf using the parameters V_{cmax}, O, and Γ (Eq. A1 in Appendix). Values of the three parameters were found by fitting rectangular hyperbola of the form $y = a\,(x - c)/(x + b)$ through the experimental $<P_N, c_i>$ points (*SigmaPlot*, v. *4.00*). The hyperbola is formally identical to Eq. A1 in Appendix ($a = V_{cmax}$, $b = O$, and $c = \Gamma$) but the values of a, b, and c found by the fitting process may differ from the values of V_{cmax} and O found in typical C_3 leaf. The reason is that we applied the fit to the whole range of experimental points up to c_i values of 600 μmol(CO_2) mol^{-1} (above the RuBPCO limitation range). Using the full c_i-scale fit, we extended the range of evaluation of the stomatal and mesophyll patchiness to the whole operation range of stomata and carboxylation. The parameters V_{cmax}, O, and Γ were estimated for the untreated plants fitting the hy-perbola through the experimental $<P_N, c_i>$ points ob-tained by manipulation of ambient CO_2 concentration. The $P_N(g_s)$ relation obtained from Eq. A3 shows the variation in P_N that would occur if $\bar{g}_s$ were independently perturbed. The derivative of the pre-stress $P_N(g_s)$ res-ponse, $\theta = \delta P_N/\delta g_s$, were calculated using equations A4a and A4b

(Appendix). Dry and low-CO_2 air provoked oscillations of $\bar{g}_s$ and P_N in the ABA-treated and, less frequently, also in control plants. We kept the environ-mental parameters and leaf temperature constant during the oscillations. We used the differences between two subsequent estimates of P_N and $\bar{g}_s$ values to approximate the θ_t derivative from the $\Delta P_N/\Delta g_s$ ratio (see Eq. A5 in Appendix).

Oxygen evolution: Five to seven days after beginning the ABA treatment, leaf discs of 10 cm^2 were cut from the 5th and 6th leaves of ABA-treated or control sunflower plants and the rate of O_2 evolution was determined at 25 °C using a *Hansatech Leaf Disc Electrode* (Norfolk, UK). Internal CO_2 concentration in the free space was either 360 or 50 000 μmol(CO_2) mol^{-1}. The CO_2 concentration was achieved by pipetting a small volume (200 to 600 mm^3) of the saturated bicarbonate solution [for 50 mmol(CO_2) mol^{-1}] or Warburg carbonate-bicarbonate mixture of appropriate composition [for 360 μmol(CO_2) mol^{-1}] onto a capillary matting. The rate of oxygen evolution in the light [300 μmol(photon) m^{-2} s^{-1}] was calculated from the linear portion of the recorded line. Amounts of the individual components of the Warburg mixture had been calculated in order that the oxygen evolution was linear with time for at least 10 min (*i.e.* consumption of less than 10 % of total carbon present in the chamber). Addition of carbonic anhydrase into the Warburg buffer did not influence the rate of oxygen evolution.

Results

Stomatal conductance and P_N in ABA-treated plants were reduced to about one half of their values in control plants (Fig. 3). Oscillations occurred more frequently in ABA-fed plants than in control plants when the leaves were exposed to dry and low-CO_2 air. In the course of the oscillations, P_N often dropped below the P_N values at equivalent c_i observed prior to the ABA treatment (Fig. 4). When g_s declined in the course of the oscillations, the inhibition of P_N [deviation from the pre-stress $P_N(c_i)$ curve, $\Delta P_N|_{ci}$] increased. During the ascending phase of g_s, $\Delta P_N|_{ci}$ diminished and reappeared during the next descending phase of g_s. These features make the oscillating plants a suitable model for analysing the cause of the reduction in P_N. Figs. 4-6 show an example of gas exchange data obtained from a single leaf before (*solid points and lines*) and 10 d after the ABA treatment (*open points*). We employed the hyperbolic regression fit (Eq. A1) to predict P_N of the untreated (pre-stressed) plant at various c_i (full line in Fig. 4). Parameters obtained from the fit [V_{cmax} = 40.2 μmol(CO_2) m^{-2} s^{-1}, Γ = 49.3 μmol(CO_2) mol^{-1}, O = 245 μmol(CO_2) mol^{-1}] were used to construct the $P_N(g_s)$ relationship for a c_a of 180 μmol(CO_2) mol^{-1} (Eq. *A*3 in Appendix, Fig. 5*A* – *full line*). After 10 d of ABA feeding, the same leaf showed oscillations of P_N and g_s when exposed to dry and low-CO_2 [180 μmol(CO_2) mol^{-1}] air (Fig. 6*A,B*). The P_N values at given $\bar{c}_i$ and $\bar{g}_s$ were lower in the ABA-treated

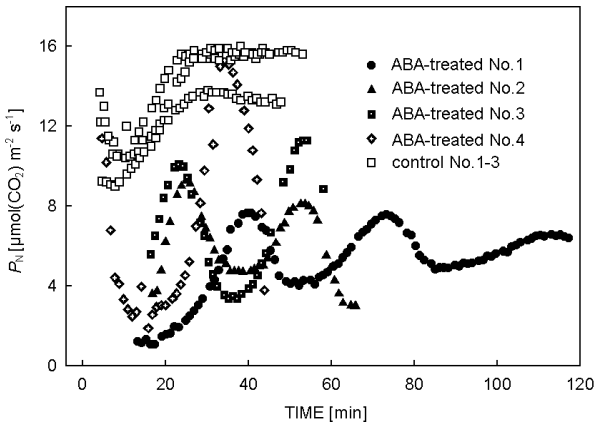

Fig. 3. Time courses of net photosynthetic rate (P_N) in three control (*open squares*) and four ABA treated (*other symbols*) sunflower plants after the leaves had been enclosed into the leaf chamber of the *LI-6400* (time zero) and supplied with dry air (0 kPa water vapour in the input air) and CO_2 concentrations of 180 (*solid circles*) or 280 (*other symbols*) μmol(CO_2) mol^{-1} in the ambient (output) air. The data from the ABA-treated plant No. 1 are analysed in Figs. 4–6. Four from 13 and three from 7 time courses, measured in ABA and control plants, respectively, are shown.

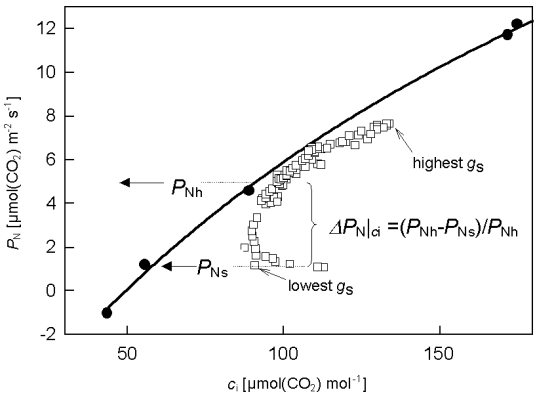

Fig. 4. The CO_2 response of photosynthesis of a single sunflower leaf before ABA treatment (*solid circles and line*) and after 10 d of plant feeding with 10^{-5} M ABA in nutrient solution (*open squares*). Parameters of the hyperbolic regression curve are: V_{cmax} = 40.2 μmol(CO_2) m^{-2} s^{-1}, Γ = 49.3 μmol(CO_2) mol^{-1}, O = 245 μmol(CO_2) mol^{-1} (see Eq. A1 in Appendix for further explanation). The variation of c_i (and g_s) in the ABA affected leaf was obtained during oscillations of gas exchange parameters shown in Fig. 6*A,B*. Ambient CO_2 concentration was 180 μmol(CO_2) mol^{-1}. Calculation of photosynthesis depression at a particular c_i ($\Delta P_N|_{ci}$) is shown.

plant than the values before ABA feeding (Figs. 4 and 5*A*). The greatest reduction of P_N at any given c_i, $\Delta P_N|_{ci}$, occurred at low g_s (Fig. 4). The inhibitions of P_N at any given $\bar{g}_s$, $\Delta P_N|_{gs}$, were less pronounced (Fig. 5A). The oscillation of E in time (not shown) produced a linear relation when plotted against g_s (Fig. 5*B*). The P_N and g_s oscillations allowed us to derive θ_t for various $\bar{g}_s$ of the oscillating leaf (Eq. A5 in Appendix) for which the pre-stress θ values were already available using Eqs. A4a,b in Appendix. Absolute values of the derivatives fluctuated between 0 and 100 μmol(CO_2) mol^{-1}(H_2O) (Fig. 6*C*). The differences of both derivatives (denoted as $\Delta\theta_t$ and calculated from Eq. 2) were near zero during the pronounced oscillatory changes of g_s, except for several negative values at very low g_s in the beginning of the time record (Fig. 6*D*). (Single points which deviated from their neighbours were ignored.)

The calculations shown above for one ABA-treated plant were done for seven investigated plants. The average parameters a, b, and c (apparent V_{cmax}, O, and Γ) measured before ABA application (day zero) were

z

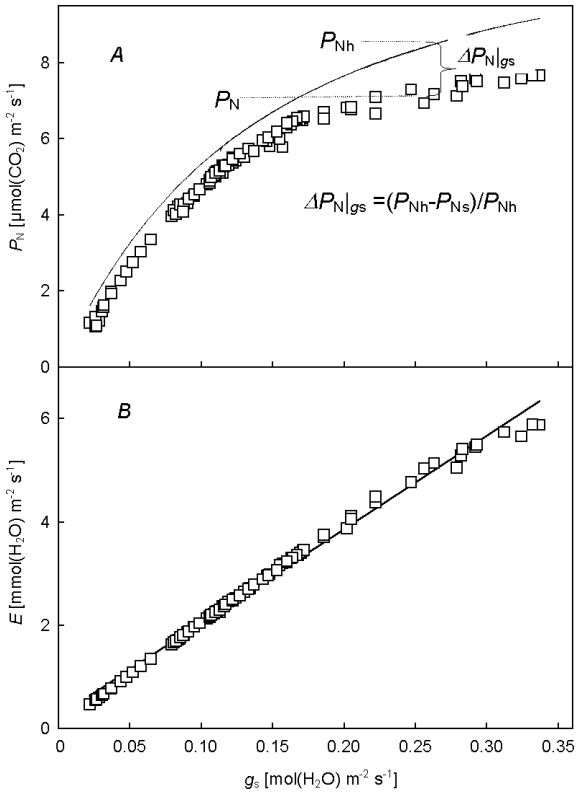

Fig. 5. Response of photosynthesis (*A*) and transpiration (*B*) to changes in stomatal conductance in the leaf before ABA treatment (*solid curve*) and after 10 d of ABA feeding (*open squares*). The P_N curve was calculated from Eq. A3 (in Appendix) using V_{cmax}, Γ, and O parameters shown in Fig. 4 and c_a 180 μmol(CO_2) mol^{-1}; the line in *B* is the linear regression line of the data. The <g_s, P_N> points shown in *A* correspond to those shown in Fig. 6*A,B*.

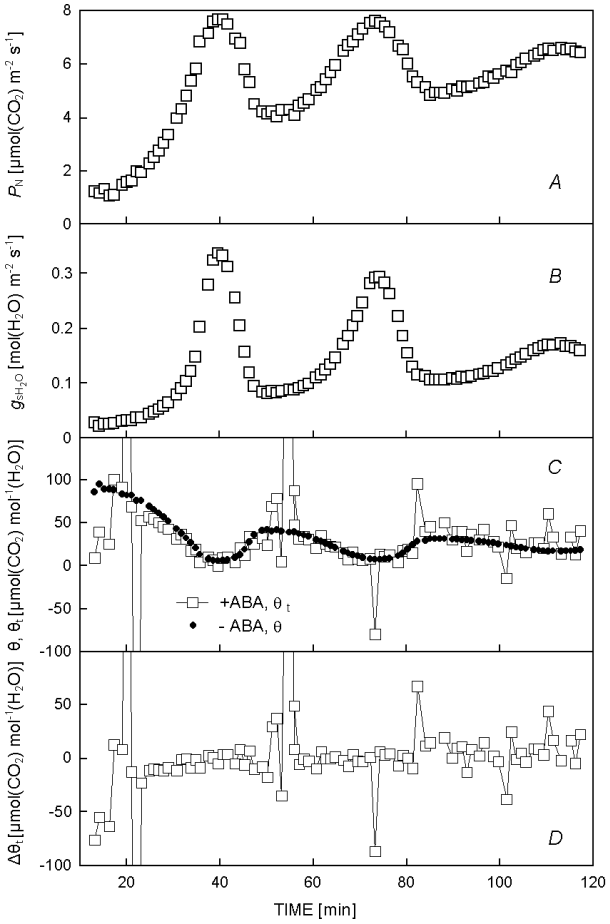

Fig. 6. Time course of net photosynthetic rate, P_N (*A*) and stomatal conductance, g_s (*B*) of an ABA-fed sunflower leaf that was enclosed in the leaf chamber at time zero (0 kPa water vapour in the input air and 180 μmol(CO_2) mol^{-1} in chamber ambient air). *C*: Time course of the sensitivity of P_N to g_s, θ, before the ABA treatment (*solid circles*) and after 10 d of ABA feeding (*open squares*). The *solid circles* represent derivatives of the line in Fig. 5*A* at the appropriate g_s and were calculated from Eqs. A4a and A4b (in Appendix). The values for the ABA treated plant (*squares*) were obtained from the points in *A* and *B* using Eq. *A*5. *D*: Total change of the sensitivity after 10 d of ABA feeding, $\Delta\theta_t$, calculated as the difference between the sensitivities shown in *C*.

36.3±5.5 μmol(CO_2) m^{-2} s^{-1}, 197.5±64.3 μmol(CO_2) mol^{-1}, and 45.6±3.5 μmol(CO_2) mol^{-1}, respectively, with coefficients of determination $r^2 > 0.99$. When exposed to dry, low CO_2 air, the four ABA-treated plants showed oscillations in all 13 measurements (3-4 measurements per plant during 10 d of ABA feeding). The three control plants yielded oscillations in three of the seven measurements only. We plotted photosynthesis inhibitions $\Delta P_N|_{ci}$ and $\Delta P_N|_{gs}$ and the sensitivity $\Delta\theta_t$ *versus* g_s. The data pooled from all time records show an increase in $\Delta P_N|_{ci}$ with stomatal closure up to 100 % (Fig. 7*A*). The $\Delta P_N|_{gs}$ inhibition rose only to 50 % with decreasing g_s, however the pattern was similar to the $\Delta P_N|_{ci}$ *versus* g_s response

(Fig. 7*B*). The inhibition rose similarly for both ABA and control plants, at least in the range of g_s measured in the control plants. In contrast, the sensitivity difference $\Delta\theta_t$ decreased at low g_s in the ABA plants, while it remained close to zero in the controls (Fig. 7*C*).

At the ambient CO_2 concentration of 50 mmol(CO_2) mol^{-1}, O_2 evolution in light did not differ between the control and ABA-influenced plants (Table 2); at 360 μmol(CO_2) mol^{-1} it was 24 % lower in plants which had been treated with ABA for 5–7 d.

Table 2. Oxygen evolution of discs from the 5th and 6th leaves of sunflower plants treated without ABA (control) or with 10^{-5} M ABA for 5 to 7 d. Distinct superscript letters denote significantly different values at $p = 0.01$. Means±SE, $n = 7$.

Ambient CO_2 concentration [μmol(CO_2) mol^{-1}]	O_2 evolution [μmol(O_2) m^{-2} s^{-1}] ABA-treated	Control
360	6.6 ± 0.5 [a]	8.7 ± 0.3 [b]
50 000	15.2 ± 0.5	16.0 ± 0.3 [b]

Discussion

Sunflower leaves exposed to dry- and low-CO_2 air exhibited oscillations in gas exchange and lowered P_N at particular c_i when compared to their humid-air $P_N(c_i)$ response. The inhibition of P_N rose at low g_s values. This effect occurred regularly in ABA-fed plants and less frequently in our control plants. There are three possible explanations for the photosynthesis inhibition. First, the biochemical capacity of the mesophyll can be reduced. Second, the <P_N, c_i> deviations can result partly from a statistically based depression in the whole-leaf photosynthesis (Fig. 1) and partly from overestimated c_i, both due to the patchy distribution of g_s. Third, omitted or underestimated cuticular conductance, g_c, can result in overestimation of c_i especially at low g_s (Meyer and Genty 1998). In the second case, P_N in stressed plants would approach to (but would not become identical with) the pre-stress $P_N(c_i)$ curve if c_i had been calculated with the heterogeneity of g_s taken into account. In conventional gas-exchange measurements, c_i is estimated as a g_s-weighted average over all local c_i and, hence, the contribution of the loci having open stomata overestimates the effective c_i (Farquhar 1989). So far, we are not able to estimate effective c_i in a leaf having non-uniformly distributed g_s. However, this effect of overestimated c_i in the apparent inhibition of P_N might be factored-out by comparing the pre- and post-stress P_N at identical g_s and c_a ($\Delta P_N|_{gs}$). However, the effect is not eliminated when c_i has been overestimated due to neglected g_c.

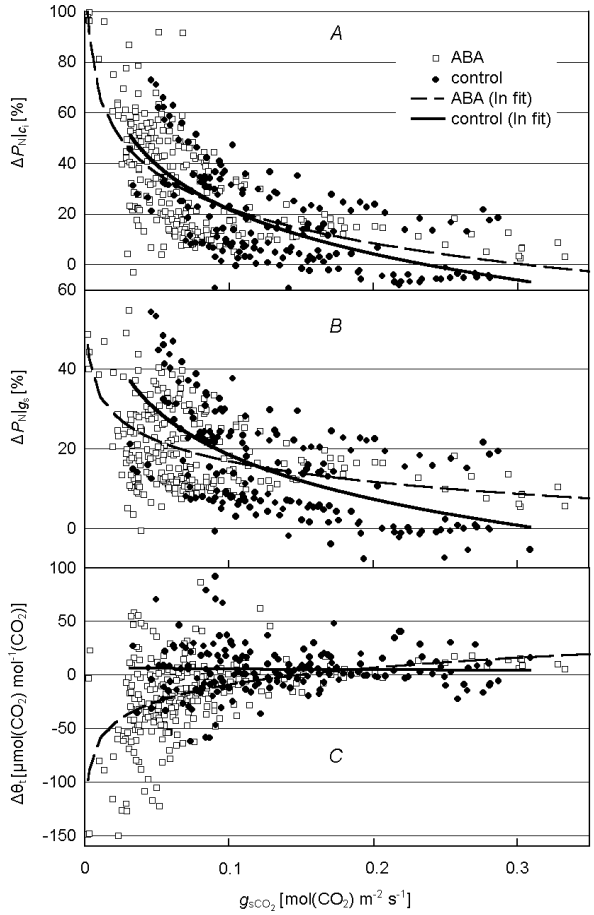

Fig. 7. Stomatal conductance dependent variations. *A*: The inhibition of photosynthesis at particular fixed c_i normalised to pre-stress values of P_N, $\Delta P_N|_{ci}$. *B*: The inhibition of photosynthesis at a particular g_s normalised to pre-stress values of P_N, $\Delta P_N|_{gs}$. *C*: The pre- and post-stress differences of the slope of P_N *versus* g_s, $\Delta\theta_t$. All were recorded during oscillations of g_s and other gas exchange parameters in three control (*closed circles*) and four ABA-fed plants (*open squares*). *The lines* represent logarithmic fits through the data points.

P_N inhibition in the selected ABA-treated plant: illusion or reality? The pre- and post-stress $P_N(g_s)$ curves were much closer than the relevant $P_N(c_i)$ curves in the selected ABA-fed plant (Figs. 4 and 5*A*). It clearly shows that the overestimation of c_i promoted the $P_N(c_i)$ deviations in Fig. 4. Thus, a large part of the deviations was an artefact of erroneously estimated c_i due to heterogeneous stomatal closure and/or due to cuticular transpiration ignored. However, the $\Delta P_N|_{gs}$ inhibitions still amounted to about 50 % at low g_s. Does the inhibition result from g_c ignored in the construction of the pre-stress $P_N(g_s)$ curve and, thus, no inhibition exists in reality or do we deal with a real inhibition resulting from heterogeneous leaf photosynthesis and mesophyll down-regulations? The effect of g_c will be reinvestigated first.

The problem has been thoroughly treated by Meyer and Genty (1998). Briefly, g_s to CO_2 is calculated from the leaf conductance to water vapour assuming both gases have identical pathways through the stomata and

boundary layer and using a constant ratio of diffusivities for water and CO_2. However, there is a parallel flux of water through the cuticle without any significant transcuticular flux of CO_2. Despite low water permeability of cuticle, this flux can exceed stomatal transpiration when stomata are nearly closed. When ignoring the cuticular flux and taking it erroneously as a stomatal flux, g_s values for both water and CO_2 are overestimated. Then, the molar fraction of CO_2 at evaporating sides inside the leaf, c_i, is also overestimated when calculated conventionally (Eq. A2 in Appendix in the simplest form). Similarly, the pre- and post-stress P_N at a particular g_s may differ when the pre-stress $P_N(g_s)$ relation has been constructed from the data obtained with an unstressed leaf having high g_s. Thus, we wonder whether the points in Fig. 5*A* would fit to the curve and $\Delta P_N|_{gs}$ become zero when g_s would be lower by a constant value of g_c. When Mayer and Genty (1998) corrected the c_i data of ABA-treated *Rosa rubiginosa* for g_c, ranging from 2 to 4 mmol(H_2O) m^{-2} s^{-1}, the $P_N(c_i)$ deviations diminished substantially. To obtain a similar effect in our plant analysed in Figs. 4 and 5, g_c has to be about 10–20 mmol(H_2O) m^{-2} s^{-1}. Then, the horizontal difference between the points and the curve in Fig. 5*A* would fully disappear, at least for g_s ranging from 0.025 to 0.100 mmol(H_2O) m^{-2} s^{-1}. The five times higher g_s value in hairy amphistomatous leaf of sunflower compared to waxy hypostomatous leaf of *Rosa* seems likely. As suggested by one of our anonymous reviewers, the rising apparent g_c (horizontal difference between the curve and points in Fig. 5*A*) at higher g_s can be explained by inhibition of maximum electron transport rate (J_{max}) in the ABA-treated plant. From above, we may summarise that the effect of neglected cuticular transpiration could explain the apparent photosynthesis inhibition shown in Figs. 4 and 5. However, this interpretation is based on an arbitrary value of cuticular transpiration that is difficult to verify experimentally with stomatous cuticles (Kerstiens 1996). Fortunately, the interference of cuticular transpiration is eliminated in the θ parameter estimated from the time changes of P_N and g_s. It makes θ insensitive to cuticular transpiration provided that g_c does not vary with time and with g_s. In addition, we showed that the deviations of θ from zero may distinguish between patchy stomata and mesophyll effects on $\Delta P_N|_{gs}$. Nevertheless, the near-zero $\Delta\theta_t$ values in Fig. 6*D* support the interpretation of g_c as the main factor creating the illusion of photosynthesis inhibition shown in Fig. 5*A*. Zero values of $\Delta\theta_t$ would indicate that, in reality, the curve and the points in Fig. 5*A* match each other.

Alternatively, we can see two other explanations for the near-zero $\Delta\theta_t$ values. First, the sensitivity of their measurements, defined as the magnitude of $\Delta\theta_t$ produced per unit of photosynthetic depression $\Delta P_N|_{gs}$, is too low to be detected by the available gas-exchange technique. Second, the mesophyll capacity of CO_2 fixation varied during the oscillations in negative proportion to the level of stomatal patchiness: when the capacity decreased, the patchiness rose so that the effects on θ were counterbalanced. As a result, we would not find any systematic deviation of $\Delta\theta_t$ from zero. The first alternative (lack of sensitivity) can be approximately assessed from Fig. 2. Reduction of V_{cmax} to one half and a bimodal distribution of g_s with modes g_{s2} and g_{s1}, each change θ by about 25 μmol(CO_2) mol^{-1}(CO_2). Each decreases P_N by about 2.5 μmol(CO_2) m^{-2} s^{-1}, *i.e.* by 30 % of its pre-stress value (Fig. 1). Thus, we can expect $\Delta\theta_t$ to vary by about +16 or –16 μmol(CO_2) mol^{-1}(H_2O) by a modest inhibition of photosynthesis (20–30 %) when patchy stomata or inhibited capacity is the single reason for the inhibition. When both act concomitantly, $\Delta\theta_t$ will approach zero from the positive or negative side. However, bimodal distribution is not the typical pattern of patchy stomata, therefore the effect of patchiness might be less than +16 μmol(CO_2) mol^{-1}(H_2O). It lead us to reinvestigate the $\Delta\theta_t$ values more thoroughly.

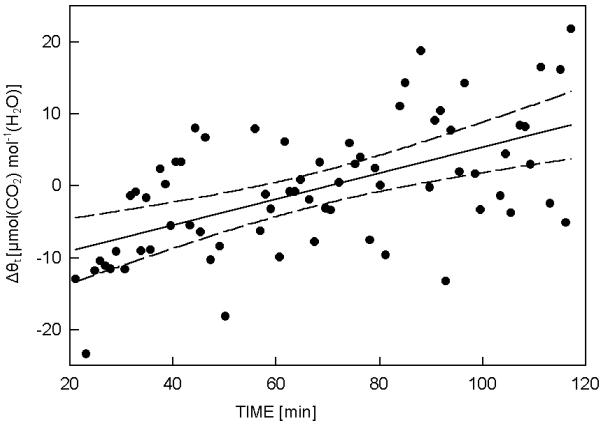

Fig. 8. Time course of the stress-induced changes in sensitivity of photosynthesis, $\Delta\theta_t$, during oscillations of stomatal conductance and photosynthesis shown in Fig. 6*A,B*. Data were taken from Fig. 6*D* ignoring the single deviating points. Regression line (solid, $r^2 = 0.33$) and 99 % confidence interval (*dashed lines*) are shown.

Looking more closely on the trend of points in Fig. 6*D*, we recognise negative $\Delta\theta_t$ at the beginning of the time record followed by a small increase of $\Delta\theta_t$ leading to positive values at the end. Ignoring the single 'spikes' in Fig. 6*D*, the values of $\Delta\theta_t$ on the regression line in Fig. 8 rose from about –10 to +10 μmol(CO_2) mol^{-1}(H_2O) between the 20th and 120th min of oscillations. It indicates that, at the beginning of oscillations, when stomata are nearly closed, an internal non-stomatal factor primarily inhibits photosynthesis while after 2 h, when the new steady states in g_s and P_N are reached, the effect of patchy stomata prevails. Higher patchiness at the steady state is consistent with observations of patches oscillating synchronously at the high-amplitude-phase of gas exchange oscillations and a transition to non-synchronous oscillations at steady state of gas exchange (Siebke and Weis 1995). The variability of $\Delta\theta_t$ estimation was rather high

(Fig. 8). Thus, the modest inhibitions of photosynthesis producing low deviations in θ must be interpreted with caution and a large number of estimates are essential. Nevertheless, the systematic increase of $\Delta\theta_t$ shown in Fig. 8 indicates that cuticular transpiration was not the only reason for P_N inhibition in the ABA treated plant. Probably both chloroplast processes at high amplitude of gas exchange oscillations and stomatal patchiness near the steady state took part in the photosynthesis inhibition.

ABA *vs.* control plants; metabolic component of the ABA effect: The extreme inhibitions of photosynthesis occurred at low g_s in both ABA and control plants (Fig. 7*A,B*). It suggests that g_c may be responsible provided that $\Delta\theta_t$ is close to zero. Despite high scatter, the logarithmic fit located the values of $\Delta\theta_t$ close to zero over the whole range of g_s in control plants. In ABA plants in contrast, $\Delta\theta_t$ dropped to negative values near stomatal closure. Thus, while a leaf internal factor probably inhibited photosynthesis in ABA-treated plants at low g_s, the inhibition in control plants could disappear with suitable cuticular conductance taken into account.

At low g_s, the steep declines of θ values in the ABA treated plants indicate that a metabolic factor was involved in the reduction of photosynthesis (Fig. 7*C*). There is mixed opinion on the effect of ABA on carboxylation capacity. While several studies indicated the existence of such an effect (Cornic and Miginiac 1983, Raschke and Hedrich 1985, Seemann and Sharkey 1987, Ward and Bunce 1987, Meyer and Genty 1999, Tezara *et al*. 1999), others did not prove any non-stomatal effect of ABA (*e.g*. Dubbe *et al*. 1978, Bradford *et al*. 1983, Lauer and Boyer 1992, Meyer and Genty 1998, Franks and Farquhar 2001). The θ-based indication of a metabolic impairment in our ABA-fed plants is consistent with the results of Meyer and Genty (1999). They identified the ABA-induced decrease in maximal electron transport rate measured during the transient saturating CO_2 pulse. The decrease was presumably caused by RuBPCO deactivation under low CO_2 availability. We detected depression of a mesophyll factor in the ABA-treated but not in the control plants exposed to similar conditions (low g_s and c_a). Thus, either the ABA effect, for example RuBPCO deactivation, was not mediated by low c_i, or c_i was less in ABA-fed than in control plants at identical g_s and c_a. We did not find any effect of ABA on oxygen production under saturated CO_2 conditions (Table 2), which indicates that the RuBPCO capacity to drive electron transport was unaffected during the steady-state measurements of oxygen production, at least. Other our attempts to detect directly a non-stomatal effect of ABA on photochemical machinery, have yielded negative results so far (not shown here). For example, we did not find any significant changes in chlorophyll *a* and *b* contents between control and ABA-treated plants after 10 d of ABA feeding. Also, the irradiance-response and $P_N(c_i)$ curves measured at steady state and high air humidity showed a similar pattern in both control and ABA-fed plants. It indicates that ABA did not accelerate leaf senescence, loss of RuBPCO, or pigment content under usual physiological conditions. In summary, it seems likely that the transient inhibition of carboxylation capacity in ABA-fed plants under low g_s and low c_a, results from some other factor(s) than the low CO_2 availability in chloroplasts. The unknown factor may cause the temporary reduction of the RuBPCO-activation state (Sage *et al*. 1990, 2002, Meyer and Genty 1999).

Stomata and mesophyll patchiness: Stomata, as a population, 'sense' the mesophyll capacity of CO_2 fixation in non-stressed plants (*e.g*. Wong *et al.* 1979, 1985, Jarvis and Davies 1998). The proportionality between mesophyll capacity and g_s indicates that a similar relationship could exist also at the scale of a single areole (heterobaric patch). For example, a group of nearly closed stomata (g_{s2} in Fig. 2) could operate next to a patch of mesophyll cells with low biochemical capacity (point B on the dashed line in Fig. 2), while the wide-open stomata (g_{s1}) could serve high-capacity chloroplasts (C on the solid line). How would this patchy mesophyll capacity (spatial non-uniformity in V_{cmax}) affect θ and our θ-based observations? It can be shown from the shape of the V_{cmax} *vs*. g_s relationship, that the uniform decrease of V_{cmax} and the evolution of a patchy pattern in V_{cmax} both produce a decrease in θ. Assuming a mechanistic coupling between mesophyll and stomata, the apparently unlikely possibility that the mesophyll inhibition compensates for the effect of stomatal-patchiness on θ seems acceptable. By using the θ parameter we cannot distinguish between the uniform and patchy pattern of the changes in mesophyll capacity so it is not possible to judge, for example, whether the spatial patterns of mesophyll capacity and the pattern of stomatal patchiness match each other. Osmond *et al*. (1999) reported impairments in photochemistry below open stomatal pores in wilting *Potentilla reptans* leaves. This indicates that the two-dimensional patterns of stomatal and mesophyll patchiness do not necessarily match each other. In contrast, Meyer and Genty (1999) showed the spatial pattern of metabolic inhibition as being determined by the spatial distribution of diffusion conductance.

In conclusion, ABA reduced g_s and made the sunflower leaves prone to oscillations in gas exchange when exposed to dry and low-CO_2 air. During the oscillations, the ABA-fed and control leaves showed transient inhibitions of photosynthesis at given values of g_s, $\Delta P_N|_{gs}$, presumably caused by (*1*) stomatal patchiness, (*2*) mesophyll impairments, and/or (*3*) cuticular conductance omitted in calculation of g_s. We found that the sensitivity of P_N to changes in g_s, $\theta = \delta P_N/\delta g_s$, can be employed in distinguishing between mesophyll and stomatal role in the stress-induced depressions $\Delta P_N|_{gs}$. Rising θ indicates stomatal patchiness while mesophyll inhibition should lower θ. A lack of the post- *minus* pre-stress differences

in θ favours the erroneous calculation of g_s or the dynamic balance between the opposite effects of mesophyll down-regulation and stomatal patchiness. In well watered, no ABA fed plants, θ did not change markedly during the $\Delta P_N|_{gs}$ depressions. It supports the idea of uniform stomatal behaviour and no metabolic inhibitions during the gas exchange oscillations in the control leaves. Alternatively, this effect could reflect an overlap in the spatial patterns of stomatal and mesophyll patchiness. However in ABA-fed plants, θ decreased at low $\bar{g}_s$, indicating an additional ABA-promoted inhibition of chloroplast processes possibly due to RuBPCO inactivation. The course of θ during a selected damp oscillation in ABA-fed plant suggests chloroplast down-regulation at the beginning of the oscillation and patchy stomatal conductance at steady state.

References

Buckley, T.N., Farquhar, G.D., Mott, K.A.: Qualitative effects of patchy stomatal conductance distribution features on gas exchange calculations. – Plant Cell Environ. **20**: 867-880, 1997.

Buckley, T.N., Mott, K.A.: Stomatal responses to non-local changes in PFD: evidence for long-distance hydraulic interactions. – Plant Cell Environ. **23**: 301-309, 2000.

Bradford, K.J., Sharkey, T.D., Farquhar, G.D.: Gas exchange, stomatal behavior, and $\delta^{13}C$ values of the *flacca* tomato mutant in relation to abscisic acid. – Plant Physiol. **72**: 245-250, 1983.

Caemmerer, S. von, Farquhar, G.D.: Some relationships between the biochemistry of photosynthesis and the gas exchange of leaves. – Planta **153**: 376-387, 1981.

Cheeseman, J.M.: PATCHY: Simulating and visualising the effects of stomatal patchiness on photosynthetic CO_2 exchange studies. – Plant Cell Environ. **14**: 593-599, 1991.

Cornic, G., Miginiac, E.: Nonstomatal inhibition of net CO_2 uptake by (±) abscisic acid in *Pharbitis nil*. – Plant Physiol. **73**: 529-533, 1983.

Downton, W.J.S., Loveys, B.R., Grant, W.J.R.: Salinity effects on the stomatal behaviour of grapevine. – New Phytol**. 116**: 499-503, 1990.

Dubbe, D.R., Farquhar, G.D., Raschke, K.: Effect of abscisic acid on the gain of the feedback loop involving carbon dioxide and stomata. – Plant Physiol. **62**: 413-417, 1978.

Farquhar, G.D.: Models of integrated photosynthesis of cells and leaves. – Phil. Trans. roy. Soc. London **B 323**: 357-367, 1989.

Farquhar, G.D., Caemmerer, S. von, Berry, J.A.: A biochemical model of photosynthetic CO_2 assimilation in leaves of C_3 species. – Planta **49**: 78-90, 1980.

Farquhar, G.D., Sharkey, T.D.: Stomatal conductance and photosynthesis. – Annu. Rev. Plant Physiol. **33**: 317-345, 1982.

Franks, P.J., Farquhar, G.D.: The effect of exogenous abscisic acid on stomatal development, stomatal mechanics, and leaf gas exchange in *Tradescantia virginiana*. – Plant Physiol. **125**: 935-942, 2001.

Haefner, J.W., Buckley, T.N., Mott, K.A.: A spatially explicit model of patchy stomatal responses to humidity. – Plant Cell Environ. **20**: 1087-1097, 1997.

Hirasawa, T., Wakabayashi, K., Touya, S., Ishihara, K.: Stomatal responses to water deficits and abscisic acid in leaves of sunflower plants (*Helianthus annuus* L.) grown under different conditions. – Plant Cell Physiol. **36**: 955-964, 1995.

Jarvis, A.J., Davies, W.J.: The coupled response of stomatal conductance to photosynthesis and transpiration. – J. exp. Bot. **49**: 399-406, 1998.

Kerstiens, G.: Diffusion of water vapour and gases across cuticles and through stomatal pores presumed closed. – In: Kerstiens, G. (ed.): Plant Cuticles – An Integrated Functional Approach. Pp. 121-134. BIOS Scientific Publishers, Oxford 1996.

Kaiser, H., Kappen, L.: Stomatal oscillations at small apertures: indications for a fundamental insufficiency of stomatal feedback-control inherent in the stomatal turgor mechanism. – J. exp. Bot. **52**: 1303-1313, 2001.

Laisk, A.: Calculation of leaf photosynthetic parameters considering the statistical distribution of stomatal apertures. – J. exp. Bot. **34**: 1627-1635, 1983.

Lange, O.L., Lösch, R., Schulze, E.-D., Kappen, L.: Responses of stomata to changes in humidity. – Planta **100**: 76-86, 1971.

Lauer, M.J., Boyer, J.: Internal CO_2 measured directly in leaves. Abscisic acid and low leaf water potential cause opposing effects. – Plant Physiol. **98**: 1310-1316, 1992.

Meyer, S., Genty, B.: Mapping intercellular CO_2 mole fraction (Ci) in *Rosa rubiginosa* leaves fed with abscisic acid using chlorophyll fluorescence imaging. Significance of Ci estimated from gas exchange. – Plant Physiol. **116**: 947-957, 1998.

Meyer, S., Genty, B.: Heterogenous inhibition of photosynthesis over the leaf surface of *Rosa rubiginosa* L. during water stress and abscisic acid treatment: induction of a metabolic component by limitation of CO_2 diffusion. – Planta **210**: 126-131, 1999.

Mott, K.A.: Effects of patchy stomatal closure on gas exchange measurements following abscisic acid treatment. – Plant Cell Environ. **16**: 1291-1300, 1995.

Mott, K.A., Buckley, T.N.: Stomatal heterogeneity. – J. exp. Bot. **49**: 407-417, 1998.

Osmond, C.B., Kramer, D., Lüttge, U.: Reversible water stress-induced non-uniform chlorophyll fluorescence quenching in wilting leaves of *Potentilla reptans* may not be due to patchy stomatal responses. – Plant Biol. **1**: 618-624, 1999.

Pospíšilová, J., Šantrůček, J.: Stomatal patchiness: effects on photosynthesis. – In: Pessarakli, M. (ed.): Handbook of Photosynthesis. Pp. 427-441. Marcel Dekker, New York – Basel – Hong Kong 1997.

Raschke, K., Hedrich, R.: Simultaneous and independent effects of abscisic acid on stomata and the photosynthetic apparatus in whole leaves. – Planta **163**: 105-118, 1985.

Sage, R.F., Cen, Y.-P., Li, M.: The activation state of Rubisco directly limits photosynthesis at low CO_2 and low O_2 partial pressures. – Photosynth. Res. **71**: 241-250, 2002.

Sage, R.F., Sharkey, T.D., Seemann, J.R.: Regulation of ribulose-1,5-bisphosphate carboxylase activity in response to light intensity and CO_2 in the C_3 annuals *Chenopodium album* L. and *Phaseolus vulgaris* L. – Plant Physiol. **94**: 1735-1742, 1990.

Seemann, J.R., Sharkey, T.D.: The effect of abscisic acid and other inhibitors on photosynthetic capacity and the biochemistry of CO_2 assimilation. – Plant Physiol. **84**: 696-700, 1987.

Sharkey, T.D., Seemann, J.R.: Mild water stress effects on carbon-reduction-cycle intermediates, ribulose bisphosphate carboxylase activity, and spatial homogeneity of photosynthesis in intact leaves. – Plant Physiol. **89**: 1060-1065, 1989.

Siebke, K., Weis, E.: Assimilation images of leaves of *Glechoma hederacea*: Analysis of non-synchronous stomata related oscillations. – Planta **196**: 155-165, 1995.

Terashima, I.: Anatomy of non-uniform leaf photosynthesis. – Photosynth. Res. **31**: 195-212, 1992.

Terashima, I., Wong, S.-C., Osmond, C.B., Farquhar, G.D.: Characterisation of non-uniform photosynthesis induced by abscisic acid in leaves having different mesophyll anatomies. – Plant Cell Environ. **29**: 385-394, 1988.

Tezara, W., Mitchell, V.J., Driscoll, S.D., Lawlor, D.W.: Water stress inhibits plant photosynthesis by decreasing coupling factor and ATP. – Nature **401**: 914-917, 1999.

Van Kraalinger, D.W.G.: Implications of non-uniform stomatal closure on gas exchange calculations. – Plant Cell Environ. **13**: 1001-1004, 1990.

Ward, D.A., Bunce, J.A.: Abscisic acid simultaneously decreases carboxylation efficiency and quantum yield in attached soybean leaves. – J. exp. Bot. **38**: 1182-1192, 1987.

Weyers, J.D.B., Lawson, T.: Heterogeneity in stomatal characteristics. – Adv. bot. Res. **26**: 317-352, 1997.

Wong, S.C., Cowan, I.R., Farquhar, G.D.: Stomatal conductance correlates with photosynthetic capacity. – Nature **282**: 424-426, 1979.

Wong, S.C., Cowan, I.R., Farquhar, G.D.: Leaf conductance in relation to rate of CO_2 assimilation. I. Influence of nitrogen nutrition, phosphorus nutrition, photon flux density, and ambient partial pressure of CO_2 during ontogeny. – Plant Physiol. **78**: 821-825, 1985.

Wullschleger, S.D.: Biochemical limitations to carbon assimilation in C_3 plants. – A retrospective analysis of the A/C_i curves from 109 species. – J. exp. Bot. **44**: 907-920, 1993.

Appendix of Equations A1 to A5

Solution for P_N at the intersection of the demand and supply functions; the first derivative of the $P_N(g_s)$ function

The RuBPCO limited net CO_2 assimilation rate, P_N, can be expressed from the biochemical model of photosynthesis (Farquhar *et al*. 1980) as

$$P_N = \frac{V_{cmax}(c_i - \Gamma)}{c_i + O} - R_D \qquad (A1),$$

where $O = K_c (1 + o/K_o)$, V_{cmax} is maximum rate of carboxylation, c_i and o are CO_2 and O_2 concentrations in chloroplasts (we assume c_i to be identical with the concentration in the sub-stomatal cavity), Γ is CO_2 compensation concentration without respiration, and K_c and K_o are Michaelis-Menten constants for CO_2 and O_2, respectively. Assumption of the inhibition of dark respiration in light ($R_D = 0$) and substitution for c_i from the simple form of CO_2 supply function,

$$c_i = c_a - \frac{P_N}{g_s} \qquad (A2),$$

yields a quadratic equation $a P_N^2 + b P_N + c = 0$ where $a = 1/g_s$, $b = -O - c_a - V_{cmax}/g_s$ and $c = V_{cmax}(c_a - \Gamma)$. Solution for P_N gives

$$P_N = \frac{1}{2} g_s \left[\frac{V_{cmax}}{g_s} + O + c_a - \sqrt{(-O - \frac{V_{cmax}}{g_s} - c_a)^2 - 4\frac{V_{cmax}(c_a - \Gamma)}{g_s}} \right] \qquad (A3).$$

Differentiation of P_N in Eq. A3 with respect to g_s gives for the first derivative:

$$\theta = \frac{\partial P_N}{\partial g_s} = \frac{P_N}{g_s} - \frac{1}{2}\frac{V_{cmax}}{g_s} - \frac{1}{2} t' g_s \qquad (A4a),$$

where t is the square root of the discriminant in the quadratic Eq. A3 [$t = (b^2 - 4\,a\,c)^{0.5}$] and its partial derivative with respect to g_s (t') is

$$t' = \frac{V_{cmax} b + 2c}{t g_s^2} \qquad (A4b).$$

The plot of θ *vs.* g_s is shown in Fig. 2. As R_D is a constant additive to P_N, the derivative P_N is not affected by the assumption of a particular (zero) value of R_D in light. This is also true for additional, constant and, with respect to g_s, in parallel arranged conductances like g_c. Further, g_s in the equations here is conductance to CO_2.

Estimation of θ_t during stomatal conductance and photosynthesis oscillations

The curvature of P_N *versus* g_s was estimated numerically from P_N and g_s values recorded during the oscillations. We used the following algorithm:

$$\theta_t = \left(\frac{\partial P_N}{\partial g_s} \right)_t \approx \frac{\Delta P_N}{\Delta g_s} = \frac{P_{N(t)} - P_{N(t+1)}}{g_{s(t)} - g_{s(t+1)}} \qquad \text{(A5)}$$

where the index t in the last term refers to time. It is possible to calculate the derivative this way only if Δg_s is sufficiently small. We learned from the simulation model (not shown here) that Δg_s should be less than 0.02 mol m^{-2} s^{-1}. The time interval was adjusted so that the increment of g_s did not exceed this limit.